Spherical Expansion of an Arbitrary Electromagnetic Field

by

Roberto Carlos Alvarez

A Thesis Presented in Partial Fulfillment
of the Requirement for the Degree
Master of Arts

Approved April 2021 by the
Graduate Supervisory Committee:

Erika T. Camacho, Co-Chair
Richard A. Kirian, Co-Chair
Malena I. Español

ARIZONA STATE UNIVERSITY

May 2021

ABSTRACT

Optical trapping schemes that exploit radiation forces, such as optical tweezers, are well understood and widely used to manipulate microparticles; however, these are typically effective only on short (sub-millimeter) length scales. In the past decade, manipulating micron sized objects over large distances ($\sim$0.5 meters) using photophoretic forces has been experimentally established. Photophoresis, discovered by Ehrenhaft in the early twentieth century, is the force a small particle feels when exposed to radiation while immersed in a gas. The anisotropic heating caused by the radiation results in a net momentum transfer on one side with the surrounding gas. To date, there is no theoretical evaluation of the photophoretic force in the case of an arbitrary illumination profile (i.e. not a plane wave) incident on a dielectric sphere, starting from Maxwell's equations. Such a treatment is needed for the case of recently published photophoretic particle manipulation schemes that utilize complicated wavefronts such as diverging Laguerre-Gaussian-Bessel beams.

Here the equations needed to determine the expansion coefficients for electromagnetic fields when represented as a superposition of spherical harmonics are derived. The algorithm of Driscoll and Healy for the efficient numerical integration of functions on the 2-sphere is applied and validated with the plane wave, whose analytic expansion is known. The expansion coefficients of the incident field are related to the field inside the sphere, from which the distribution of heat deposition can be evaluated. The incident beam is also related to the scattered field, from which the scattering forces may be evaluated through the Maxwell stress tensor. In future work, these results will be combined with heat diffusion/convection simulations within the sphere and a surrounding gas to predict the total forces on the sphere, which will be compared against experimental observations that so far remain unexplained.

TABLE OF CONTENTS

Page

APPENDIX Page

LIST OF TABLES

Table Page

LIST OF FIGURES

Chapter 1

INTRODUCTION

1.1 Background

The near atomic resolution of x-rays has enabled imaging nanometer and sub-nanometer particles through crystallographic methods. Traditional crystallography requires crystallized samples and returns only static structures. Worse still, the ionizing nature of x-rays irreparably damages chemical bonds – vaporizing small molecules, like proteins. However, recent innovations have allowed for new experimental techniques that mitigate these limitations.

Simulations by Neutze, Neutze *et al.* (2000), suggested the possibility of imaging individual particles by exposing them to an intense x-ray beam ($\sim 10^6$ photons per angstrom^2) for a short amount of time ($\sim 10^{-15}$ s). The idea is to gather structural data before the radiation can alter the target's structure. The advent of the x-ray free electron laser (XFEL), capable of providing femtosecond pulses, made the "diffraction-before-destruction" paradigm experimentally viable.

Chapman, Chapman *et al.* (2006), imaged a synthetic target made of silicon nitride with "soft" (relatively long wavelength) x-rays at the Free-electron LASer (FLASH) in Germany. The reconstructed image, while low resolution, showed no signs of radiation damage; scanning electron microscope imaging before exposure confirmed the reconstruction and post exposure revealed extensive radiation damage on the target, confirming diffraction-before-destruction. Also at FLASH, Bogan, Bogan *et al.* (2008), imaged a nanoscale particle in free flight – an important prerequisite towards imaging uncrystallized biomolecules.

Due to their sub-nanometer resolution hard x-rays (relatively short wavelength) are preferable to soft x-rays for single particle imaging (SPI) experiments; however, imaging objects significantly smaller than viruses, such as proteins, is limited by the number of scattered photons – typically only a few hundred. Thus, image reconstruction requires millions of diffraction patterns. To overcome this, SPI experiments need to increase the number of scattering interactions with dense target beams.

Current sample delivery research efforts concentrate on aerodynamic focusing by aerodynamic lensing or convergent nozzle. Aerodynamic lens stacks consist of a series of concentric axis-symmetric apertures that focus particles by balancing inertial and drag forces. Aerodynamic lensing is capable of creating dense beams for varying particle sizes – tens to hundreds of micrometers, Kirian *et al.* (2015). Convergent nozzles join two capillaries inside a nozzle, one carrying liquid sample and one filled with focusing gas. Gas dynamic virtual nozzles (GDVN) are capable of generating dense sample beams less than 10 microns in diameter, Nazari *et al.* (2020), but continuous sample delivery is costly – especially for expensive or hard to produce targets. These methods have successfully been implemented at many experiments; however, they lack precise control over the spatial position of the sample.

1.2 The Photophoretic Force

In the early twentieth century Ehrenhaft, Ehrenhaft (1917), reported on the movement of small particles when exposed on one side to sufficiently intense light, he called this the photophoretic force. When anisotropically illuminated, a small particle will heat non-uniformly and consequently have a greater heat (momentum) transfer on one side, causing a net force (photophoretic) in one direction. Recently the photophoretic force was used to successfully manipulate, Shvedov *et al.* (2010), micron sized particles over meter long distances. Following this development, Eckerskorn, Eckerskorn

et al. (2015), proposed using the photophoretic force for SPI sample delivery.

The method proposed by Eckerskorn is to use a hollow optical laser beam to trap and deliver particles precisely to the XFEL beam. To our knowledge, there is no model that unifies photophoretic and shorter range gradient based trapping schemes, such as optical tweezers. Here we provide a model from Maxwell's equations that allows us to calculate the spherical harmonic expansion of an arbitrary initial electromagnetic field. In future work this can be combined with a heat diffusion model to describe the photophoretic force.

Chapter 2

MAXWELL'S EQUATIONS

James Clerk Maxwell produced a comprehensive and consistent mathematical review of the experimental observations of electric and magnetic phenomena. This work was refined by Oliver Heaviside and Heinrich Hertz to four coupled partial differential equations. Maxwell's equations encode the physical laws of electrodynamics – the theoretical framework unifying electricity, magnetism, and optics.

2.1 The Microscopic Equations

The sources of electromagnetic phenomena are charges, currents, and changes in the electric ($\mathbf{E} \in \mathbb{R}^3$) or magnetic ($\mathbf{B} \in \mathbb{R}^3$) fields. Maxwell's equations,

$$\boldsymbol{\nabla} \cdot \mathbf{E} = \frac{\rho}{\varepsilon_0} \tag{2.1a}$$

$$\boldsymbol{\nabla} \cdot \mathbf{B} = 0 \tag{2.1b}$$

$$\boldsymbol{\nabla} \times \mathbf{E} + \frac{\partial \mathbf{B}}{\partial t} = 0 \tag{2.1c}$$

$$\boldsymbol{\nabla} \times \mathbf{B} - \mu_0 \varepsilon_0 \frac{\partial \mathbf{E}}{\partial t} = \mu_0 \mathbf{J}, \tag{2.1d}$$

relate the fields to their sources, Griffiths (2013). Electric and magnetic fields are omnipresent, but the charge ($\rho \in \mathbb{R}$) and current ($\mathbf{J} \in \mathbb{R}^3$) density are localized. In SI units, the permittivity and permeability of free space, $\epsilon_0 = 8.85418782 \times 10^{-12}\mathrm{A}^2\mathrm{s}^4\mathrm{kg}^{-1}\mathrm{m}^{-3}$ and $\mu_0 = 1.25663706 \times 10^{-6}\mathrm{mA}^{-2}\mathrm{s}^{-2}\mathrm{kg}$, are the proportionality constants.

In this work we will only consider an uncharged sphere with no currents. Generally the electric and magnetic fields may depend on position and time – we will assume

time harmonic fields, that is

$$\mathbf{E}(\mathbf{r},t) = \mathrm{Re}\big\{\mathbf{E}_c(\mathbf{r})e^{-i\omega t}\big\} \quad \text{and} \quad \mathbf{B}(\mathbf{r},t) = \mathrm{Re}\big\{\mathbf{B}_c(\mathbf{r})e^{-i\omega t}\big\}$$

where ω is an angular frequency and the complex, position dependent, fields must satisfy

$$\boldsymbol{\nabla}\cdot\mathbf{E}_c = 0 \tag{2.2a}$$

$$\boldsymbol{\nabla}\cdot\mathbf{B}_c = 0 \tag{2.2b}$$

$$\boldsymbol{\nabla}\times\mathbf{E}_c = i\omega\mathbf{B}_c \tag{2.2c}$$

$$\boldsymbol{\nabla}\times\mathbf{B}_c = -i\mu_0\varepsilon_0\omega\mathbf{E}_c. \tag{2.2d}$$

Equations (2.2a) to (2.2d) are justified by assuming $\mathbf{E}(\mathbf{r},t)$ and $\mathbf{B}(\mathbf{r},t)$ may be expanded as a Fourier series in time, i.e. general electric and magnetic fields are the superposition of all frequencies

$$\mathbf{E}(\mathbf{r},t) = \mathrm{Re}\bigg\{\int \mathrm{d}\omega\ \mathbf{E}_c(\mathbf{r})e^{-i\omega t}\bigg\} \tag{2.3}$$

$$\mathbf{B}(\mathbf{r},t) = \mathrm{Re}\bigg\{\int \mathrm{d}\omega\ \mathbf{B}_c(\mathbf{r})e^{-i\omega t}\bigg\}. \tag{2.4}$$

For this to be allowable the fields must be integrable and have at most a finite number of discontinuities – these are reasonable restrictions on physically realizable fields.

Combining eqs. (2.2c) and (2.2d) $\mathbf{E}_c$ or $\mathbf{B}_c$ can be eliminated (see Appendix A). Eliminating $\mathbf{B}_c$ and setting $k^2 = \mu_0\varepsilon_0\omega^2$ we arrive at the Helmholtz equation

$$\nabla^2\mathbf{E}_c + k^2\mathbf{E}_c = 0 \tag{2.5}$$

constrained by $\boldsymbol{\nabla}\cdot\mathbf{E}_c = 0$ with $\mathbf{B}_c = -(i/\omega)\boldsymbol{\nabla}\times\mathbf{E}_c$; alternatively, we arrive at

$$\nabla^2\mathbf{B}_c + k^2\mathbf{B}_c = 0 \tag{2.6}$$

constrained by $\boldsymbol{\nabla}\cdot\mathbf{B}_c = 0$ with $\mathbf{E}_c = (i/\omega)\boldsymbol{\nabla}\times\mathbf{B}_c$ if $\mathbf{E}_c$ is eliminated. Either of these two are equivalent to eqs. (2.2a) to (2.2d). In the rest of this work we will

assume electromagnetic fields to be time-harmonic and drop the subscript c with the understanding that physically realizable fields are always the real part of the complex equations.

2.2 The Macroscopic Equations

The electric and magnetic fields are inconvenient to describe the fields created by electric charges and currents inside bulk matter. The electric displacement $\mathbf{D}$ and magnetic displacement $\mathbf{H}$ fields, sometimes called the auxiliary fields, are more suitable and satisfy Maxwell's equations.

In a dielectric the total charge density is, Griffiths (2013),

$$\rho = \rho_f + \rho_b = \rho_f - \boldsymbol{\nabla} \cdot \mathbf{P}. \tag{2.7}$$

Plugging eq. (2.7) into eq. (2.1a) we can see that

$$\boldsymbol{\nabla} \cdot (\epsilon_0 \mathbf{E} + \mathbf{P}) = \rho_f \tag{2.8}$$

where $\mathbf{P} \in \mathbb{R}^3$ is the polarization of the material and the electric displacement field is defined as

$$\mathbf{D} = \epsilon_0 \mathbf{E} + \mathbf{P}. \tag{2.9}$$

Similarly, the total current density in a dielectric is

$$\mathbf{J} = \mathbf{J}_f + \mathbf{J}_b = \mathbf{J}_f + \boldsymbol{\nabla} \times \mathbf{M} \tag{2.10}$$

where $\mathbf{M} \in \mathbb{R}^3$ is the magnetization of the material, Griffiths (2013). Plugging eq. (2.10) into eq. (2.1d) we arrive at

$$\boldsymbol{\nabla} \times \left(\frac{1}{\mu_0} \mathbf{B} - \mathbf{M} \right) = \mathbf{J}_f, \tag{2.11}$$

with the magnetic displacement field defined as

$$\mathbf{H} = \frac{1}{\mu_0} \mathbf{B} - \mathbf{M}. \tag{2.12}$$

The polarization and magnetization may have any complicated form, but they must satisfy the material Maxwell's equations, Jackson (1999). In a domain without free charge or current sources and the time dependence given by $e^{-i\omega t}$, $\mathbf{D}$ and $\mathbf{H}$ satisfy

$$\begin{array}{ccc} \boldsymbol{\nabla} \cdot \mathbf{D} = 0 & & \boldsymbol{\nabla} \cdot \mathbf{B} = 0 \\ & \text{and} & \\ \boldsymbol{\nabla} \times \mathbf{E} = i\omega \mathbf{B} & & \boldsymbol{\nabla} \times \mathbf{H} = -i\omega \mathbf{D} \end{array} .$$

If $\mathbf{P}$ ($\mathbf{M}$) relates linearly to $\mathbf{E}$ ($\mathbf{B}$) then the material is called linear. Assuming a linear material that is moreover isotropic and homogeneous, the constitutive relations are $\mathbf{P} = \epsilon_0 \chi_e \mathbf{E}$ and $\mathbf{M} = \mu_0 \chi_m \mathbf{H}$ where the electric, $\chi_e \in \mathbb{R}$, and magnetic, $\chi_m \in \mathbb{R}$, susceptibilities are proportionality constants that are measured experimentally and are independent of the field position and direction, Griffiths (2013). Thus the displacement fields are

$$\mathbf{D} = \epsilon_0 (1 + \chi_e) \mathbf{E} = \epsilon \mathbf{E} \qquad \text{and} \qquad \mathbf{H} = \frac{1}{\mu_0 + \mu_0 \chi_m} \mathbf{B} = \frac{1}{\mu} \mathbf{B},$$

with $\epsilon \in \mathbb{R}$ and $\mu \in \mathbb{R}$ denoting the material permittivity and permeability. The auxiliary fields also satisfy the Helmholtz equation under these assumptions.

Moving forward, we will be using the Helmholtz equation, eq. (2.5), that was previously developed for the case of a vacuum, but with the substitution $k = \sqrt{\epsilon \mu}\omega$. We always assume that the materials are isotropic, homogeneous, and linear. Note that the ϵ and μ can be complex numbers in the case that the material absorbs electromagnetic energy.

Chapter 3

THE HELMHOLTZ EQUATION

The eigenvalue problem of the Laplace operator, $(\nabla^2 + k^2)\,\psi = 0$, is the Helmholtz equation. Given suitable boundary conditions the Helmholtz equation has a unique solution which depends continuously on the initial data.

3.1 The Helmholtz Equation in Spherical Polar Coordinates

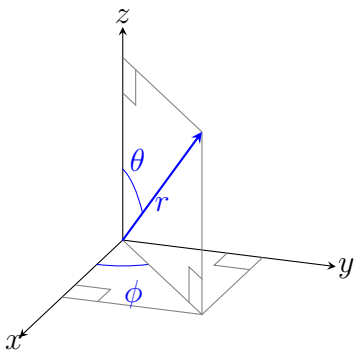

Figure 3.1: Definition of $(r,\, \theta,\, \phi)$ with Respect to Cartesian Coordinates

We use spherical coordinates with polar angle θ and azimuthal angle ϕ, with this convention the unit vectors are

$$\hat{\mathbf{e}}_r = \sin(\theta)\cos(\phi)\hat{\mathbf{e}}_x + \sin(\theta)\sin(\phi)\hat{\mathbf{e}}_y + \cos(\theta)\hat{\mathbf{e}}_z \tag{3.1}$$

$$\hat{\mathbf{e}}_\theta = \cos(\theta)\cos(\phi)\hat{\mathbf{e}}_x + \cos(\theta)\sin(\phi)\hat{\mathbf{e}}_y - \sin(\theta)\hat{\mathbf{e}}_z \tag{3.2}$$

$$\hat{\mathbf{e}}_\phi = -\sin(\phi)\hat{\mathbf{e}}_x + \cos(\phi)\hat{\mathbf{e}}_y. \tag{3.3}$$

The Helmholtz equation is

$$\frac{1}{r^2}\frac{\partial}{\partial r}\left(r^2\frac{\partial\psi}{\partial r}\right) + \frac{1}{r^2\sin(\theta)}\frac{\partial}{\partial\theta}\left(\sin(\theta)\frac{\partial\psi}{\partial\theta}\right) + \frac{1}{r^2\sin^2(\theta)}\frac{\partial^2\psi}{\partial\phi^2} + k^2\psi = 0 \tag{3.4}$$

in these coordinates and is separable such that $\psi(r,\theta,\phi) = \psi_r(r)\psi_\theta(\theta)\psi_\phi(\phi)$ (see Appendix B).

3.2 Solutions of the Helmholtz Equation

The azimuthal component satisfies the harmonic oscillator equation,

$$\frac{\mathrm{d}^2}{\mathrm{d}\phi^2}\psi_\phi + m^2\psi_\phi = 0, \tag{3.5}$$

where m is a separation constant. Equation (3.5) is solved by a linear combination of $\cos(m\phi)$ and $\sin(m\phi)$. For positive integers $m \neq n$, $\cos(m\phi)$ and $\cos(n\phi)$, $\sin(m\phi)$ and $\sin(n\phi)$, and $\cos(m\phi)$ and $\sin(n\phi)$ are orthogonal on $[0, 2\pi]$ – i.e.

$$\begin{aligned}
\int_0^{2\pi} \mathrm{d}\phi \;\; \cos(m\phi)\cos(n\phi) &= \pi\delta_{m,n} \\
\int_0^{2\pi} \mathrm{d}\phi \;\; \sin(m\phi)\sin(n\phi) &= \pi\delta_{m,n} \\
\int_0^{2\pi} \mathrm{d}\phi \;\; \cos(m\phi)\sin(n\phi) &= 0
\end{aligned}$$

where $\delta_{m,n} = 1$ if $m = n$ and 0 otherwise.

The polar component becomes, Bohren and Huffman (1983),

$$\frac{1}{\sin(\theta)}\frac{\mathrm{d}}{\mathrm{d}\theta}\left[\sin(\theta)\frac{\mathrm{d}}{\mathrm{d}\theta}\psi_\theta\right] + \left[\ell(\ell+1) - \frac{m^2}{\sin^2(\theta)}\right]\psi_\theta = 0 \tag{3.6}$$

with a second separation constant ℓ. Equation (3.6) is solved by the associated Legendre functions,

$$P_\ell^m(x) = \frac{(-1)^{\ell+m}}{2^\ell \ell!}(1-x^2)^{m/2}\frac{\mathrm{d}^{\ell+m}}{\mathrm{d}x^{\ell+m}}\left(x^2-1\right)^\ell, \tag{3.7}$$

where $x = \cos(\theta)$. $m \in \mathbb{N}$ is referred to as the order and $\ell \in \mathbb{N}$ is called the degree of the associated Legendre function. The first six associated Legendre functions are:

$$\begin{aligned}
P_0^0 &= 1 \\
P_1^0 &= \cos(\theta) \\
P_1^1 &= -\sin(\theta) \\
P_2^0 &= \frac{1}{2}\left[3\cos^2(\theta) - 1\right] \\
P_2^1 &= -3\sin(\theta)\cos(\theta) \\
P_2^2 &= 3\sin^2(\theta)
\end{aligned}$$

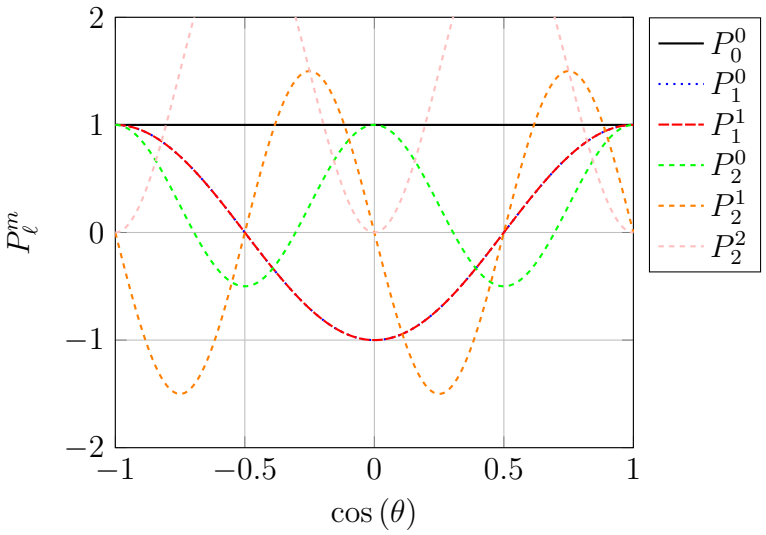

Figure 3.2: Plots of $P_\ell^m(\cos\theta)$ for $\ell, m \in \{0, 1, 2\}$ and $\theta \in [0, 2\pi]$.

For fixed order m the associated Legendre functions are orthogonal on $[-1, 1]$ with respect to degree (DLMF, 2021, Eq. 14.17.6),

$$\int_{-1}^{1} \mathrm{d}x \; P_\ell^m(x) P_n^m(x) = \frac{(\ell+m)!}{(\ell+\frac{1}{2})(\ell-m)!}\delta_{\ell,n} \; ,$$

and for fixed degree ℓ the associated Legendre function are orthogonal on $[-1, 1]$ with respect to order (DLMF, 2021, Eq. 14.17.8),

$$\int_{-1}^{1} \mathrm{d}x \; \frac{P_\ell^n(x) P_\ell^m(x)}{1-x^2} = \frac{(\ell+m)!}{m(\ell-m)!}\delta_{n,m} \; .$$

The radial component satisfies

$$\frac{\mathrm{d}}{\mathrm{d}r}\left(r^2 \frac{\mathrm{d}}{\mathrm{d}r}\psi_r\right) + [k^2 r^2 - \ell(\ell+1)]\psi_r = 0, \tag{3.8}$$

with $k \in \mathbb{C}$. We can rewrite eq. (3.8) as

$$\rho \frac{\mathrm{d}}{\mathrm{d}\rho}\left(\rho \frac{\mathrm{d}}{\mathrm{d}\rho} Z\right) + \left[\rho^2 - \left(\ell + \frac{1}{2}\right)^2\right] Z = 0 \tag{3.9}$$

by transforming to the dimensionless variable $\rho = kr$ and function $Z = \psi_r(\rho/k)\sqrt{\rho}$, Bohren and Huffman (1983). Equation (3.9) is solved by a linear combination of

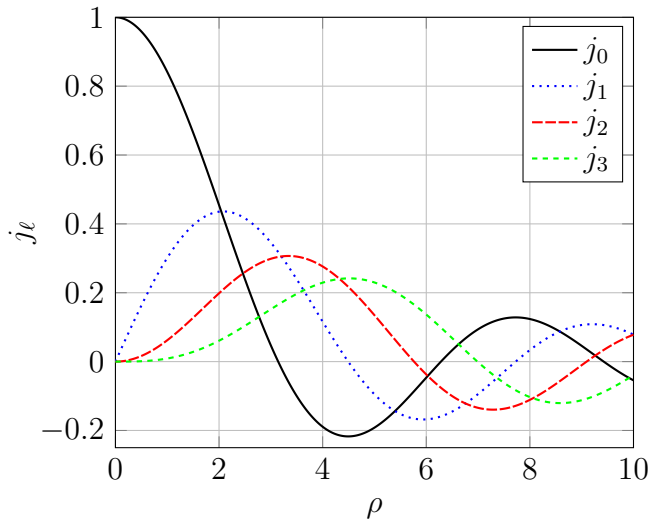

Figure 3.3: Plots of j_ℓ for $\ell \in \{0, 1, 2, 3\}$ and $\rho \in [0, 10]$.

spherical Bessel functions of the first,

$$j_\ell(\rho) = \sqrt{\frac{\pi}{2\rho}} J_\nu(\rho) = \left(\frac{\rho}{2}\right)^\nu \sum_{k=0}^{\infty} (-1)^k \frac{(\rho^2/4)^k}{k!(\nu + k)!} \quad \text{where} \quad \nu = \ell + \frac{1}{2}\,, \tag{3.10}$$

second,

$$y_\ell(\rho) = \sqrt{\frac{\pi}{2\rho}} Y_\nu(\rho) = \frac{J_\nu(\rho)\cos(\nu\pi) - J_{-\nu}(\rho)}{\sin(\nu\pi)} \tag{3.11}$$

and third kind. The latter are also known as the spherical Hankel functions of the first,

$$h_\ell^{(1)}(\rho) = j_\ell(\rho) + i y_\ell(\rho), \tag{3.12}$$

and second,

$$h_\ell^{(2)}(\rho) = j_\ell(\rho) - i y_\ell(\rho), \tag{3.13}$$

kind.

The spherical Bessel functions of the first kind, eq. (3.10), and second kind, eq. (3.11), are also known as the Bessel functions of half-integer order. J_ν and Y_ν are the Bessel functions of the first and second kind. The first three spherical Bessel

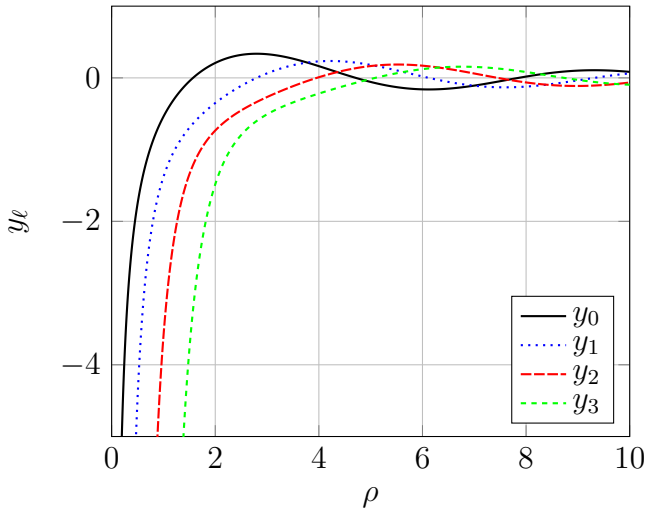

Figure 3.4: Plots of y_ℓ for $\ell \in \{0, 1, 2, 3\}$ and $\rho \in [0, 10]$.

functions of the first and second kind are

$$j_0 = \frac{\sin(\rho)}{\rho} \qquad y_0 = -\frac{\cos(\rho)}{\rho}$$

$$j_1 = \frac{\sin(\rho)}{\rho^2} - \frac{\cos(\rho)}{\rho} \qquad y_1 = -\frac{\cos(\rho)}{\rho^2} - \frac{\sin(\rho)}{\rho}$$

$$j_2 = \left(-\frac{1}{\rho} + \frac{3}{\rho^3}\right)\sin(\rho) - \frac{3}{\rho^2}\cos(\rho) \qquad y_2 = \left(-\frac{1}{\rho} + \frac{3}{\rho^3}\right)\cos(\rho) - \frac{3}{\rho^2}\sin(\rho)$$

Theorem 3.2.1. *In spherical polar coordinates the Helmholtz equation is solved by a linear combination of*

$$\psi^e_{\ell,m} = \cos(m\phi) P^m_\ell\{\cos(\theta)\} z_\ell(\rho) \tag{3.14}$$

$$\psi^o_{\ell,m} = \sin(m\phi) P^m_\ell\{\cos(\theta)\} z_\ell(\rho), \tag{3.15}$$

where $z_\ell(\rho)$ is one of the spherical Bessel functions, as determined by boundary data; $\psi^e_{\ell,m}$ is called the even and $\psi^o_{\ell,m}$ the odd solution because of the parity of the trigonometric functions, Bohren and Huffman (1983).

3.3 Spherical Harmonics

Often the angular components are combined into the spherical harmonics

$$Y_{\ell,m}(\theta,\phi) = \sqrt{\frac{2\ell+1}{4\pi}\frac{(\ell-m)!}{(\ell+m)!}} e^{im\phi} P_\ell^m\{\cos(\theta)\} \tag{3.16}$$

which are orthonormal on the unit sphere (DLMF, 2021, Eq. 14.30.8):

$$\int_0^{2\pi} \mathrm{d}\phi \int_0^{\pi} \mathrm{d}\theta \ \sin(\theta) Y^*_{\ell,m}(\theta,\phi) Y_{k,n}(\theta,\phi) = \delta_{\ell,k}\delta_{m,n} \ . \tag{3.17}$$

The spherical harmonics are eigenfunctions of L^2, which is the angular component of ∇^2 in spherical coordinates:

$$\nabla^2 f = \frac{1}{r}\frac{\partial^2}{\partial r^2}(rf) - \frac{L^2}{r^2} f.$$

We can also write $L^2 = \mathbf{L}\cdot\mathbf{L}$, where the differential operator $\mathbf{L}$ is

$$\mathbf{L} = -i(\mathbf{r}\times\boldsymbol{\nabla}) = \frac{i}{\sin(\theta)}\frac{\partial}{\partial\phi}\hat{\mathbf{e}}_\theta - i\frac{\partial}{\partial\theta}\hat{\mathbf{e}}_\phi \ . \tag{3.18}$$

The $\mathbf{L}$ operator is used often in physics because it is closely related to the angular momentum operator in quantum mechanics. Some additional useful definitions are, Jackson (1999),

$$\begin{aligned} L_\pm &= L_x \pm iL_y \\ L^2 Y_{\ell,m} &= \ell(\ell+1) Y_{\ell,m} \\ L_\pm Y_{\ell,m} &= \sqrt{(\ell\mp m)(\ell\pm m+1)}\, Y_{\ell,m+1} \\ L_z Y_{\ell,m} &= m Y_{\ell,m}. \end{aligned}$$

Theorem 3.3.1. *In spherical polar coordinates the Helmholtz equation is solved by a linear combination of*

$$\psi_{\ell,m} = z_\ell(\rho) Y_{\ell,m}(\theta,\phi) \tag{3.19}$$

where $z_\ell(\rho)$ is one of the spherical Bessel functions, as determined by boundary data, Jackson (1999).

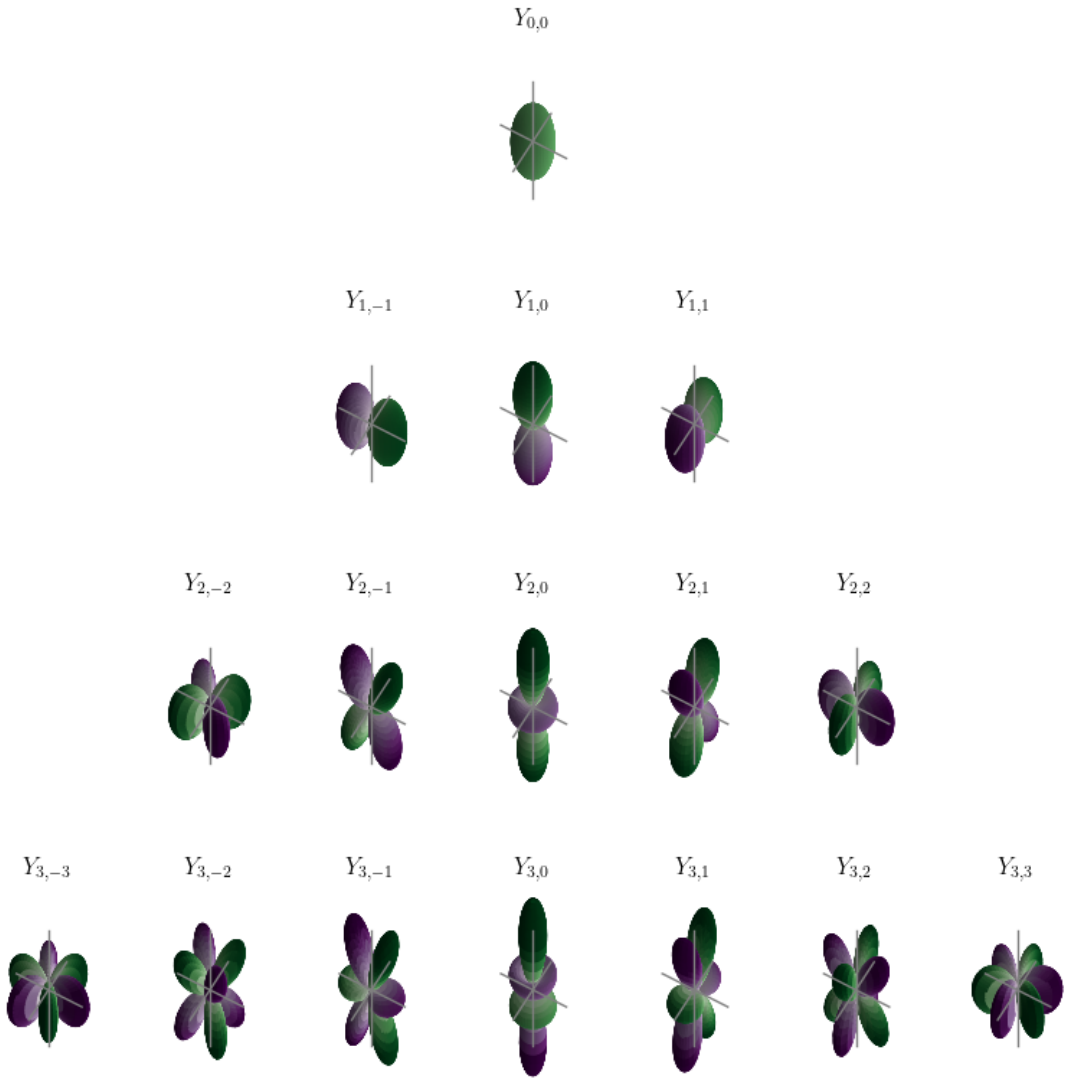

Figure 3.5: Visualization of the Real Part of $Y_\ell^m(\theta, \phi)$ for $\theta \in [0, \pi]$, $\phi \in [0, 2\pi]$, $\ell \in \{0, 1, 2, 3\}$ and $m \leq |\ell|$.

Chapter 4

THE MODEL

The solutions of Maxwell's equations that describe the absorption and scattering of a plane wave by an uncharged dielectric sphere of arbitrary radius and refractive index are generally attributed to Mie. Here we generalize the Mie solutions for an arbitrary electromagnetic wave.

4.1 Electrodynamics in Spherical Coordinates

The origin of the spherical polar coordinate system will be the center of a single uncharged dielectric sphere of radius a. Denote the set of all points in the sphere as Ω and the set of all points in the boundary as $\partial\Omega \subseteq \Omega$. In chapter 2 we demonstrated an electromagnetic wave in an ideal material satisfies

$$\nabla^2\mathbf{E} + k^2\mathbf{E} = 0 \tag{4.1}$$

where $k^2 = \mu\epsilon\omega^2$, $\boldsymbol{\nabla} \cdot \mathbf{E} = 0$, and

$$\mathbf{B} = -\frac{i}{\omega}\boldsymbol{\nabla} \times \mathbf{E}. \tag{4.2}$$

We solved eq. (4.1) for the scalar case in chapter 3, see theorem 3.3.1; there are two approaches we could take to solve the vector equation: solve for each component of $\mathbf{E}$ individually, or build up vector solutions from the scalar solution. These are equivalent, we will do the latter.

Theorem. *If ψ satisfies $\nabla^2\psi + k^2\psi = 0$, then*

$$\mathbf{M} = \boldsymbol{\nabla} \times \mathbf{r}\psi \tag{4.3}$$

satisfies $\nabla^2\mathbf{M} + k^2\mathbf{M} = 0$ *and*

$$\mathbf{N} = \frac{1}{k}\boldsymbol{\nabla} \times \mathbf{M} \tag{4.4}$$

satisfies $\nabla^2\mathbf{N} + k^2\mathbf{N} = 0$.

Proof.

$$\begin{aligned}
\nabla^2\mathbf{M} + k^2\mathbf{M} &= \nabla^2(\boldsymbol{\nabla} \times \mathbf{r}\psi) + k^2(\boldsymbol{\nabla} \times \mathbf{r}\psi) \\
&= \boldsymbol{\nabla} \times \mathbf{r}\nabla^2\psi + \boldsymbol{\nabla} \times \mathbf{r}k^2\psi \\
&= \boldsymbol{\nabla} \times \mathbf{r}(\nabla^2\psi + k^2\psi) \\
&= 0
\end{aligned}$$

$$\begin{aligned}
\nabla^2\mathbf{N} + k^2\mathbf{N} &= \nabla^2\left(\frac{1}{k}\boldsymbol{\nabla} \times \mathbf{M}\right) + k^2\left(\frac{1}{k}\boldsymbol{\nabla} \times \mathbf{M}\right) \\
&= \frac{1}{k}\left[\boldsymbol{\nabla} \times \nabla^2\mathbf{M} + \boldsymbol{\nabla} \times k^2\mathbf{M}\right] \\
&= \frac{1}{k}\left[\boldsymbol{\nabla} \times \left(\nabla^2\mathbf{M} + k^2\mathbf{M}\right)\right] \\
&= 0
\end{aligned}$$

□

Theorem. $\mathbf{N}$ *and* $\mathbf{M}$ *as defined in eqs.* (4.3) *and* (4.4) *satisfy*

$$\boldsymbol{\nabla} \cdot \mathbf{N} = 0$$

$$\boldsymbol{\nabla} \cdot \mathbf{M} = 0.$$

Proof.

$$\boldsymbol{\nabla} \cdot \mathbf{M} = \boldsymbol{\nabla} \cdot (\boldsymbol{\nabla} \times \mathbf{r}\psi) = 0 \quad \text{and} \quad \boldsymbol{\nabla} \cdot \mathbf{N} = \boldsymbol{\nabla} \cdot \left(\frac{1}{k}\boldsymbol{\nabla} \times \mathbf{M}\right) = 0.$$

□

Theorem 4.1.1.

$$\mathbf{M} = i\mathbf{L}\psi \tag{4.5}$$

$$\mathbf{N} = \frac{i}{k}\boldsymbol{\nabla} \times \mathbf{L}\psi \tag{4.6}$$

are equivalent to eqs. (4.3) *and* (4.4)*.*

Proof.

$$\begin{aligned} \mathbf{M} &= \boldsymbol{\nabla} \times \mathbf{r}\psi & \mathbf{N} &= \frac{1}{k}\boldsymbol{\nabla} \times \mathbf{M} \\ &= -\mathbf{r} \times \boldsymbol{\nabla}\psi & &= \frac{1}{k}\boldsymbol{\nabla} \times i\mathbf{L}\psi \\ &= i\mathbf{L}\psi & &= \frac{i}{k}\boldsymbol{\nabla} \times \mathbf{L}\psi \end{aligned}$$

□

Since $\mathbf{M}$ and $\mathbf{N}$ satisfy all the requirements to describe electric and magnetic fields, we may expand them as

$$\mathbf{E} = \sum_{\ell,m} \left[\alpha_{\ell,m}\mathbf{M}_{\ell,m} + \beta_{\ell,m}\mathbf{N}_{\ell,m}\right] \tag{4.7}$$

$$\mathbf{B} = -\frac{i}{\omega}\sum_{\ell,m} \left[\alpha_{\ell,m}\mathbf{N}_{\ell,m} + \beta_{\ell,m}\mathbf{M}_{\ell,m}\right] \tag{4.8}$$

where

$$\mathbf{M}_{\ell,m} = \boldsymbol{\nabla} \times \mathbf{r}\psi_{\ell,m} = i\mathbf{L}\psi_{\ell,m} \tag{4.9}$$

$$\mathbf{N}_{\ell,m} = \frac{1}{k}\boldsymbol{\nabla} \times \mathbf{M}_{\ell,m} = \frac{i}{k}\boldsymbol{\nabla} \times \mathbf{L}\psi_{\ell,m} \tag{4.10}$$

and the expansion coefficients are

$$\alpha_{\ell,m} z_\ell(kr) = \frac{-i}{\ell(\ell+1)} \int \mathrm{d}\Omega \, (\mathbf{L} \cdot \mathbf{E}) \, Y^*_{\ell,m}(\theta,\phi) \tag{4.11}$$

$$\beta_{\ell,m} z_\ell(kr) = \frac{\omega}{\ell(\ell+1)} \int \mathrm{d}\Omega \, (\mathbf{L} \cdot \mathbf{B}) \, Y^*_{\ell,m}(\theta,\phi). \tag{4.12}$$

The most general possible solution has a radial function that is a linear combination of the spherical Hankel functions, that is

$$z_\ell = A_1 h^{(1)}_\ell + A_2 h^{(2)}_\ell.$$

4.2 The Incident, Internal, and Scattered Field

The incident and internal fields must be finite everywhere, thus the radial dependence is given by the spherical Bessel function of the first kind. The incident field is

$$\mathbf{E}_0 = \sum_{\ell,m} \left[\alpha^0_{\ell,m}\mathbf{M}^0_{\ell,m} + \beta^0_{\ell,m}\mathbf{N}^0_{\ell,m}\right] \tag{4.13}$$

$$\mathbf{B}_0 = -\frac{i}{\omega}\sum_{\ell,m} \left[\alpha^0_{\ell,m}\mathbf{N}^0_{\ell,m} + \beta^0_{\ell,m}\mathbf{M}^0_{\ell,m}\right] \tag{4.14}$$

with

$$\psi^0_{\ell,m} = j_\ell(kr)Y_{\ell,m}(\theta,\phi)$$

and the expansion coefficients are given by eqs. (4.11) and (4.12) with $z_\ell(kr) = j_\ell(kr)$. The internal field is

$$\mathbf{D}_i = \epsilon\sum_{\ell,m} \left[\alpha^i_{\ell,m}\mathbf{M}^i_{\ell,m} + \beta^i_{\ell,m}\mathbf{N}^i_{\ell,m}\right] \tag{4.15}$$

$$\mathbf{H}_i = -\frac{i}{\omega\mu}\sum_{\ell,m} \left[\alpha^i_{\ell,m}\mathbf{N}^i_{\ell,m} + \beta^i_{\ell,m}\mathbf{M}^i_{\ell,m}\right] \tag{4.16}$$

with

$$\psi^i_{\ell,m} = j_\ell(knr)Y_{\ell,m}(\theta,\phi)$$

where $n = \sqrt{\epsilon/\epsilon_0}$ is the index of refraction of the sphere.

The scattered field does not see the interior of the sphere and so the radial dependence can be given by the spherical Hankel functions. Considering the asymptotic expansion

$$h^{(1)}_\ell(kr) \sim (-i)^{n-1}\frac{e^{ikr}}{kr}$$
$$h^{(2)}_\ell(kr) \sim i^{n-1}\frac{e^{-ikr}}{kr}\ ,$$

we choose $h_\ell^{(1)}$ since it corresponds to an outgoing wave at large distance from the source ($kr \gg n^2$), Bohren and Huffman (1983). The scattered field is

$$\mathbf{E}_s = \sum_{\ell,m} \left[\alpha^s_{\ell,m}\mathbf{M}^s_{\ell,m} + \beta^s_{\ell,m}\mathbf{N}^s_{\ell,m}\right] \tag{4.17}$$

$$\mathbf{B}_s = -\frac{i}{\omega}\sum_{\ell,m} \left[\alpha^s_{\ell,m}\mathbf{N}^s_{\ell,m} + \beta^s_{\ell,m}\mathbf{M}^s_{\ell,m}\right] \tag{4.18}$$

where

$$\psi^s_{\ell,m} = h_\ell^{(1)}(kr)Y_{\ell,m}(\theta,\phi).$$

The internal and scattered fields coefficients are calculated from the boundary conditions. Physically realizable electric and magnetic fields must satisfy Maxwell's equations throughout the domain. If there are no free charges or free currents at $\partial\Omega$ then the solutions inside ($r \in \Omega$) and outside ($r \notin \Omega$) must match. The material properties of the sphere are discontinuous, however we will assume the change is over a small enough distance that we can mathematically model the change as

$$n(r) = \begin{cases} \sqrt{\epsilon/\epsilon_0}, & r \in \Omega \\ 0, & r \notin \Omega \end{cases}.$$

Thus, assuming $\mu = \mu_0$, the boundary conditions are

$$\left[\mathbf{E}_0(\mathbf{r}) + \mathbf{E}_s(\mathbf{r}) - n^2(r)\mathbf{E}_i(\mathbf{r})\right] \cdot \hat{\mathbf{r}} = 0 \tag{4.19}$$

$$\left[\mathbf{B}_0(\mathbf{r}) + \mathbf{B}_s(\mathbf{r}) - \mathbf{B}_i(\mathbf{r})\right] \cdot \hat{\mathbf{r}} = 0 \tag{4.20}$$

$$\left[\mathbf{E}_0(\mathbf{r}) + \mathbf{E}_s(\mathbf{r}) - \mathbf{E}_i(\mathbf{r})\right] \times \hat{\mathbf{r}} = 0 \tag{4.21}$$

$$\left[\mathbf{B}_0(\mathbf{r}) + \mathbf{B}_s(\mathbf{r}) - \mathbf{B}_i(\mathbf{r})\right] \times \hat{\mathbf{r}} = 0. \tag{4.22}$$

Applying the boundary conditions at $r = a$ we use eq. (3.18) and

$$\boldsymbol{\nabla} \times \mathbf{L} = -\frac{i}{r}\left[\frac{\partial^2}{\partial\theta^2} + \frac{1}{\sin^2(\theta)}\frac{\partial^2}{\partial\phi^2}\right]\hat{\mathbf{e}}_r + i\frac{\partial}{\partial r}\frac{\partial}{\partial\theta}\hat{\mathbf{e}}_\theta + \frac{i}{\sin(\theta)}\frac{\partial}{\partial r}\frac{\partial}{\partial\phi}\hat{\mathbf{e}}_\phi \tag{4.23}$$

to arrive at

$$\alpha^0_{\ell,m} j_\ell(ka) = \alpha^i_{\ell,m} j_\ell(kna) - \alpha^s_{\ell,m} h^{(1)}_\ell(ka) \tag{4.24}$$

$$\alpha^0_{\ell,m} \frac{\partial}{\partial a}\left[a\ j_\ell(ka)\right] = \alpha^i_{\ell,m} \frac{\partial}{\partial a}\left[a\ j_\ell(kna)\right] - \alpha^s_{\ell,m} \frac{\partial}{\partial a}\left[a\ h^{(1)}_\ell(ka)\right] \tag{4.25}$$

and

$$\beta^0_{\ell,m} j_\ell(ka) = n^2(r)\beta^i_{\ell,m} j_\ell(kna) - \beta^s_{\ell,m} h^{(1)}_\ell(ka) \tag{4.26}$$

$$\beta^0_{\ell,m} \frac{\partial}{\partial a}\left[a\ j_\ell(ka)\right] = \beta^i_{\ell,m} \frac{\partial}{\partial a}\left[a\ j_\ell(knr)\right] - \beta^s_{\ell,m} \frac{\partial}{\partial a}\left[a\ h^{(1)}_{\ell,m}(ka)\right]. \tag{4.27}$$

Rewriting the systems of equations as matrix equations,

$$\alpha^0_{\ell,m} \begin{pmatrix} j_\ell(ka) \\ \frac{\partial}{\partial a}\left[a\ j_\ell(ka)\right] \end{pmatrix} = \begin{pmatrix} j_\ell(kna) & -h^{(1)}_\ell(ka) \\ \frac{\partial}{\partial a}\left[a\ j_\ell(kna)\right] & -\frac{\partial}{\partial a}\left[a\ h^{(1)}_\ell(ka)\right] \end{pmatrix} \begin{pmatrix} \alpha^i_{\ell,m} \\ \alpha^s_{\ell,m} \end{pmatrix} \tag{4.28}$$

$$\beta^0_{\ell,m} \begin{pmatrix} j_\ell(ka) \\ \frac{\partial}{\partial a}\left[a\ j_\ell(ka)\right] \end{pmatrix} = \begin{pmatrix} n^2(r) j_\ell(kna) & -h^{(1)}_\ell(ka) \\ \frac{\partial}{\partial a}\left[a\ j_\ell(kna)\right] & -\frac{\partial}{\partial a}\left[a\ h^{(1)}_\ell(ka)\right] \end{pmatrix} \begin{pmatrix} \beta^i_{\ell,m} \\ \beta^s_{\ell,m} \end{pmatrix}, \tag{4.29}$$

we can solve for the internal and scattered field coefficients,

$$\begin{pmatrix} \alpha^i_{\ell,m} \\ \alpha^s_{\ell,m} \end{pmatrix} = \frac{\alpha^0_{\ell,m}}{d} \begin{pmatrix} -\frac{\partial}{\partial a}\left[a\ h^{(1)}_\ell(ka)\right] & h^{(1)}_\ell(ka) \\ -\frac{\partial}{\partial a}\left[a\ j_\ell(kna)\right] & j_\ell(kna) \end{pmatrix} \begin{pmatrix} j_\ell(ka) \\ \frac{\partial}{\partial a}\left[a\ j_\ell(kna)\right] \end{pmatrix} \tag{4.30}$$

$$\begin{pmatrix} \beta^i_{\ell,m} \\ \beta^s_{\ell,m} \end{pmatrix} = \frac{\beta^0_{\ell,m}}{d} \begin{pmatrix} -\frac{\partial}{\partial a}\left[a\ h^{(1)}_\ell(ka)\right] & h^{(1)}_\ell(ka) \\ -\frac{\partial}{\partial a}\left[a\ j_\ell(kna)\right] & n^2(r) j_\ell(kna) \end{pmatrix} \begin{pmatrix} j_\ell(ka) \\ \frac{\partial}{\partial a}\left[a\ j_\ell(kna)\right] \end{pmatrix} \tag{4.31}$$

where

$$d = h^{(1)}_\ell(ka) \frac{\partial}{\partial a}\left[a\ j_\ell(kna)\right] - j_\ell(kna) \frac{\partial}{\partial a}\left[a h^{(1)}_\ell(ka)\right].$$

Here is the core of our model. Given an electric field at some point in space the magnetic field can be calculated from eq. (4.2), we can compute the spherical expansion from eqs. (4.11) and (4.12), $\alpha^0_{\ell,m}$ and $\beta^0_{\ell,m}$ from eq. (4.30) and eq. (4.31). The index of refraction n and the radius r of the sphere is all we need to compute the

scattered and internal fields once we have the incident field expansion coefficients. From these we can compute any quantity of interest. This model depends on the calculation of the angular integrals eqs. (4.11) and (4.12).

4.3 Mie Theory

The spherical expansion of a scalar plane wave is

$$e^{i\mathbf{k}\cdot\mathbf{r}} = \sum_{\ell=0}^{\infty} i^{\ell}(2\ell+1) j_{\ell}(kr) P_{\ell}(\cos\gamma) \tag{4.32}$$

and since $P_{\ell} \propto Y_{\ell,0}$ we can write

$$e^{i\mathbf{k}\cdot\mathbf{r}} = \sum_{\ell=0}^{\infty} i^{\ell}\sqrt{4\pi(2\ell+1)}\, j_{\ell}(kr) Y_{\ell,0}(\gamma), \tag{4.33}$$

where γ is the angle between $\mathbf{k}$ and $\mathbf{r}$, Jackson (1999). Now consider a circularly polarized plane wave propagating along the z-axis

$$\mathbf{E}_0 = e^{i\mathbf{k}\cdot\mathbf{r}}[\hat{\mathbf{e}}_x + i\hat{\mathbf{e}}_y] \tag{4.34}$$

$$\mathbf{B}_0 = -\frac{i}{\omega}\mathbf{E}_0. \tag{4.35}$$

With eqs. (4.33) and (4.34) we compute

$$\begin{aligned}
\alpha^0_{\ell,m} j_{\ell}(kr) &= \frac{-i}{\ell(\ell+1)} \int \mathrm{d}\Omega\ \mathbf{L}\cdot\mathbf{E}_0 Y^*_{\ell,m} \\
&= \frac{-i}{\ell(\ell+1)} \int \mathrm{d}\Omega\ \mathbf{L}\cdot[\hat{\mathbf{e}}_x + i\hat{\mathbf{e}}_y]\, e^{i\mathbf{k}\cdot\mathbf{r}} Y^*_{\ell,m}(\theta,\phi) \\
&= \frac{-i}{\ell(\ell+1)} \sum_{\ell=0}^{\infty} i^{\ell}\sqrt{4\pi(2\ell+1)}\, j_{\ell}(kr) \int \mathrm{d}\Omega\ \left[L_x + iL_y\right] Y_{\ell,0}(\theta,\phi) Y^*_{\ell,m}(\theta,\phi) \\
&= \frac{-i}{\ell(\ell+1)} \sum_{\ell=0}^{\infty} i^{\ell}\sqrt{4\pi(2\ell+1)}\, j_{\ell}(kr) \int \mathrm{d}\Omega\ L_+ Y_{\ell,0}(\theta,\phi) Y^*_{\ell,m}(\theta,\phi);
\end{aligned}$$

applying the raising operator L_+

$$\begin{aligned}
\alpha^0_{\ell,m} j_{\ell}(kr) &= \frac{-i}{\ell(\ell+1)} \sum_{\ell=0}^{\infty} i^{\ell}\sqrt{4\pi(2\ell+1)\ell(\ell+1)}\, j_{\ell}(kr) \int \mathrm{d}\Omega\ Y^*_{\ell,m}(\theta,\phi) Y_{\ell,1}(\theta,\phi) \\
&= -i^{\ell+1}\frac{\sqrt{4\pi(2\ell+1)}}{\sqrt{\ell(\ell+1)}} j_{\ell}(kr)\delta_{\ell,\ell}\delta_{m,1}
\end{aligned}$$

we can see

$$\alpha^0_{\ell,1} = -i^{\ell+1}\sqrt{\frac{4\pi(2\ell+1)}{\ell(\ell+1)}} \tag{4.36}$$

and

$$\beta^0_{\ell,1} = -i\alpha^0_{\ell,1} = -i^{\ell}\sqrt{\frac{4\pi(2\ell+1)}{\ell(\ell+1)}}\ . \tag{4.37}$$

4.4 Spherical Harmonic Expansion

For a function f defined on the 2-sphere if the radial and angular components can be decoupled – that is $f(r,\theta,\phi) = g(r)f'(\theta,\phi)$ – then the spherical harmonic expansion of f is

$$f(r,\theta,\phi) = \sum_{\ell=0}^{\infty}\sum_{m=0}^{\ell}\alpha_{\ell,m}g_{\ell,m}(r)Y_{\ell,m}(\theta,\phi), \tag{4.38}$$

where

$$\alpha_{\ell,m}g_{\ell,m}(r) = \int \mathrm{d}\Omega\ Y^*_{\ell,m}(\theta,\phi)f'(\theta,\phi). \tag{4.39}$$

Functions on the 2-sphere that are integrable can be expanded in spherical harmonics, but we need an efficient numerical algorithm to compute eq. (4.39) for any arbitrary function. We use the algorithm of Driscoll and Healy.

Theorem. *For a band limited function, that is*

$$f(\theta,\phi) = \sum_{\ell=0}^{L}\sum_{m=0}^{\ell}\alpha_{\ell,m}Y_{\ell,m}(\theta,\phi),$$

$$a_{\ell,m} = \int \mathrm{d}\Omega\ Y^*_{\ell,m}(\theta,\phi)f(\theta,\phi) = \sum_{h=0}^{2L+1}\sum_{j=0}^{2L+1}Y^*_{\ell,m}(\theta_j,\phi_h)f(\theta_j,\phi_h)w_j \tag{4.40}$$

with weights

$$w_j = \frac{4\pi}{2(L+1)^2}\sin\left[\frac{(2j+1)\pi}{4(L+1)}\right]\sum_{i=0}^{L}\left(\frac{1}{2i+1}\right)\sin\left[\frac{(2j+1)(2i+1)\pi}{4(L+1)}\right], \tag{4.41}$$

sampled at

$$\theta_j = \left(j+\frac{1}{2}\right)\frac{\pi}{2L+2} \quad \text{and} \quad \phi_h = \frac{h\pi}{L+1}. \tag{4.42}$$

Equation (4.40) is exact, in exact arithmetic, Driscoll and Healy (1994).

Chapter 5

RESULTS AND DISCUSSION

5.1 Results

We tested the Driscoll and Healy algorithm by checking the orthonormality of the spherical harmonics. The program was written in Python and tested on a machine with floating point precision of 15 decimal places ($\epsilon_m = 2.220446049250313 \times 10^{-16}$). Figure (5.1) plots the results of the numerical integration of $Y_{\ell,\ell}$ for $\ell \in [0, 50]$. Table (5.1) is an excerpt from the automated tests.

$Y^*_{\ell,m} Y_{\ell,m}$	Answer	Driscoll Healy
$Y^*_{0,0} Y_{0,0}$	1	$0.9999999999(999983)$
$Y^*_{1,0} Y_{1,0}$	1	$0.9999999999(999994)$
$Y^*_{1,1} Y_{1,1}$	1	$0.9999999999(999998)$
$Y^*_{0,0} Y_{1,1}$	0	$-3.7947076036(992655) \times 10^{-17}$

Table 5.1: Results: Testing Orthonormality of Spherical Harmonics with the Driscoll Healy Algorithm.

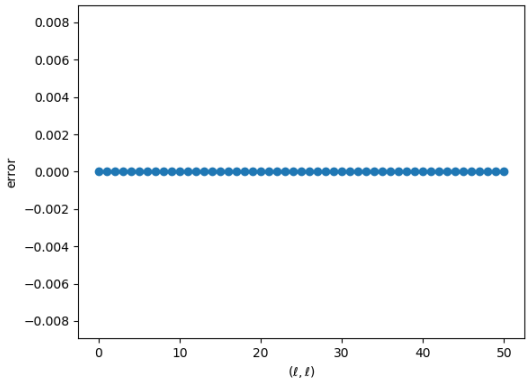

Figure 5.1: Results: Testing Spherical Harmonic Orthonormality with the Driscoll Healy Algorithm ($L = 50$).

The results of integrating a scalar planewave along the z-axis,

$$\begin{aligned}\int \mathrm{d}\Omega\ e^{i\hat{\mathbf{e}}_z\cdot\mathbf{r}} &= \int_0^{2\pi}\mathrm{d}\phi\int_0^{\pi}\mathrm{d}\theta\ \sin(\theta)e^{ir\cos(\theta)}\\ &= 2\pi\int_{-1}^{1}\mathrm{d}\cos(\theta)\ e^{ir\cos(\theta)}\\ &= 2\pi\frac{\sin(r)}{r}\ ,\end{aligned}$$

are presented in figure (5.2) for $r = 10$ and $\ell \in [0, 25]$.

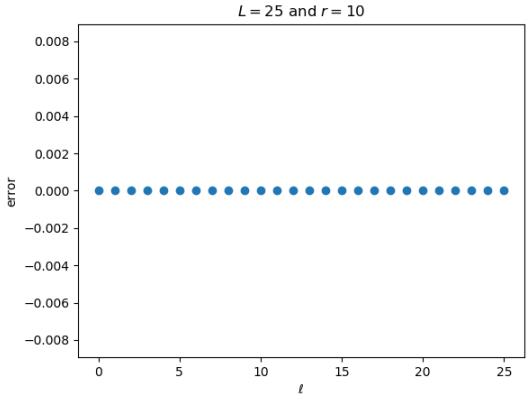

Figure 5.2: Results: Testing Integration with the Driscoll Healy Algorithm of Scalar Planewave along z-axis ($L = 25$).

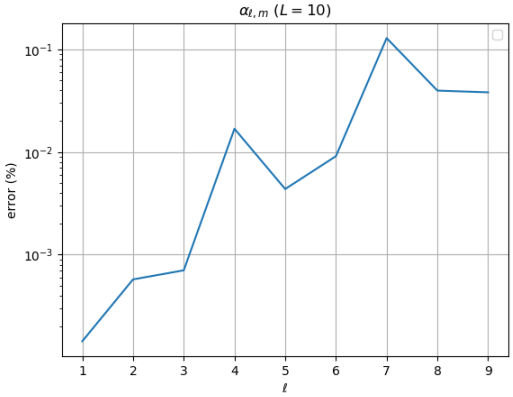

Figure 5.3: Results: Testing Integration with the Driscoll Healy Algorithm of Vector Planewave along z-axis ($L = 10$).

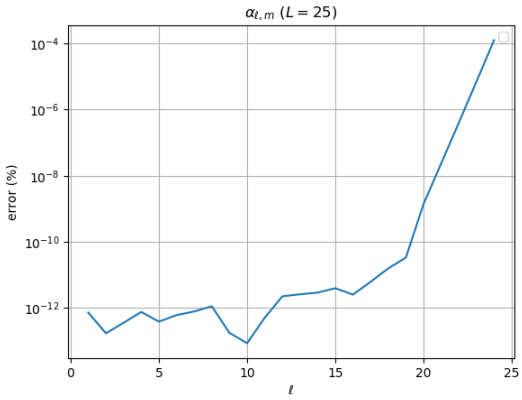

Figure 5.4: Results: Testing Integration with the Driscoll Healy Algorithm of Vector Planewave along z-axis ($L = 25$).

5.2 Discussion

Our tests were designed to consider 10 matching decimal places (rounded) passing and any number smaller than ϵ_m to be 0. This was mainly for two reasons: 6 significant figures can be easily achieved experimentally and to account for errors in the numerical algorithms that generate the spherical harmonics and spherical bessel functions. From table (5.1) we can see that the first few orthonormality relations are indeed satisfied. Figure (5.1) is a stronger indication of the success of the Driscoll Healy algorithm, with the computed error 0 for all $Y_{\ell,\ell}$, $\ell \in [0, 50]$. The scalar planewave was also successfully integrated to the correct answer with the algorithm up to $L = 25$.

To recreate the Mie solution we simulated a circularly polarized planewave (eq. 4.34) with a wavelength of 532 nm (green light) traveling along the z-axis and incident on a 1 μm sphere. For $L = 10$ (figure 5.3) we can see that the maximum error is $\sim 0.1\%$ at $\ell = 7$, however increasing $L = 25$ (figure 5.4) the maximum error is $\sim 0.0001\%$ at $\ell = 25$ with the error at $\ell = 7$ reduced to $\sim 10^{-12}\%$. This indicates that the primary source of error is truncation error. A secondary source of error

comes from the numerical calculation of the spherical Bessel functions.

The spherical Bessel functions are typically computed from a recurrence relation. The forward direction (i.e. $j_\ell \to j_{\ell+1}$) is numerically unstable so often the values are generated in the reverse direction. One approach is to assume that some large ℓ is 0 and $\ell-1$ is 1 then work down to j_0 from the recursion and then apply a normalization condition such as

$$j_0 + 2\sum_{m=1}^{\infty} j_{2m} = 1, \tag{5.1}$$

Stegun and Abramowitz (1957), but this method introduces truncation error. An alternative approach is to use some asymptotic expansion of the spherical Bessel functions and recurse backwards from that. The fidelity of this method depends on how good of an approximation the asymptotic expression is. In the analytic derivation of the Mie expansion coefficients eqs. (4.36) and (4.37) we could cancel out the spherical Bessel functions on both sides, however we cannot do that numerically. We could divide over the spherical Bessel functions and compute

$$\alpha^0_{\ell,m} = \frac{-i}{\ell(\ell+1)j_\ell(kr)} \int \mathrm{d}\Omega \, (\mathbf{L}\cdot\mathbf{E}_0)\, Y^*_{\ell,m}(\theta,\phi); \tag{5.2}$$

but, since $j_\ell \to 0$ for large order or argument we can quickly begin dividing by 0.

The success of the algorithm to integrate not only $Y_{\ell,m}$ but also the scalar planewave $e^{-ir\cos(\theta)}$ and compute the Mie expansion coefficents of a vector planewave with a maximum error of $\sim 0.0001\%$ for $L = 25$ leads us to conclude that the expansion coefficients of an arbitrary initial electromagnetic field can be computed numerically. Additionally, the primary sources of error were identified and are within the acceptable limit, i.e. they do not affect 10 significant figures.

In the previous chapter we derived matrix equations – eqs. (4.28) and (4.29) – for the expansion coefficents of the internal and scattered fields, which are solved by eqs. (4.30) and (4.31) and depend on the radius and index of refraction of the sphere

as well as $\alpha^0_{\ell,m}$ and $\beta^0_{\ell,m}$. Therefore, we can completely characterize the electric and magnetic fields everywhere. From this description we can compute many quantities of interest. For example, the energy deposited into the sphere and with the material properties we can derive the heat distribution inside the sphere; or the scattering force on the sphere by integrating the Maxwell stress tensor over an appropiate surface. Combining this with a heat diffusion model we can predict the photophoretic force, thus accounting for all forces on the sphere, allowing us to predict its trajectory.

REFERENCES

Abramowitz, M., I. A. Stegun and R. H. Romer, *Handbook of mathematical functions with formulas, graphs, and mathematical tables* (American Association of Physics Teachers, 1988).

Bogan, M. J., W. H. Benner, S. Boutet, U. Rohner, M. Frank, A. Barty, M. M. Seibert, F. Maia, S. Marchesini, S. Bajt *et al.*, "Single particle x-ray diffractive imaging", Nano letters **8**, 1, 310–316 (2008).

Bohren, C. F. and D. R. Huffman, *Absorption and Scattering of Light by Small Particles* (John Wiley & Sons, 1983).

Chapman, H. N., A. Barty, M. J. Bogan, S. Boutet, M. Frank, S. P. Hau-Riege, S. Marchesini, B. W. Woods, S. Bajt, W. H. Benner *et al.*, "Femtosecond diffractive imaging with a soft-x-ray free-electron laser", Nature Physics **2**, 12, 839–843 (2006).

DLMF, "*NIST Digital Library of Mathematical Functions*", http://dlmf.nist.gov/, Release 1.1.1 of 2021-03-15, URL `http://dlmf.nist.gov/`, f. W. J. Olver, A. B. Olde Daalhuis, D. W. Lozier, B. I. Schneider, R. F. Boisvert, C. W. Clark, B. R. Miller, B. V. Saunders, H. S. Cohl, and M. A. McClain, eds. (2021).

Driscoll, J. R. and D. M. Healy, "Computing fourier transforms and convolutions on the 2-sphere", Advances in Applied Mathematics **15**, 2, 202–250 (1994).

Eckerskorn, N., R. Bowman, R. A. Kirian, S. Awel, M. Wiedorn, J. Küpper, M. J. Padgett, H. N. Chapman and A. V. Rode, "Optically induced forces imposed in an optical funnel on a stream of particles in air or vacuum", Phys. Rev. Applied **4**, 064001, URL `https://link.aps.org/doi/10.1103/PhysRevApplied.4.064001` (2015).

Ehrenhaft, F., "On the physics of millionths of centimeters", Phys. Z. **18**, 352–368 (1917).

Griffiths, D. J., *Introduction to Electrodynamics* (Pearson, 2013).

Jackson, J. D., *Classical Electrodynamics* (John Wiley & Sons, Inc., 1999).

Kirian, R., S. Awel, N. Eckerskorn, H. Fleckenstein, M. Wiedorn, L. Adriano, S. Bajt, M. Barthelmess, R. Bean, K. Beyerlein *et al.*, "Simple convergent-nozzle aerosol injector for single-particle diffractive imaging with x-ray free-electron lasers", Structural Dynamics **2**, 4, 041717 (2015).

Marsden, J. E. and A. Tromba, *Vector Calculus* (Macmillan, 2003).

Nazari, R., S. Zaare, R. C. Alvarez, K. Karpos, T. Engelman, C. Madsen, G. Nelson, J. C. Spence, U. Weierstall, R. J. Adrian *et al.*, "3d printing of gas-dynamic virtual nozzles and optical characterization of high-speed microjets", Optics Express **28**, 15, 21749–21765 (2020).

Neutze, R., R. Wouts, D. Van der Spoel, E. Weckert and J. Hajdu, "Potential for biomolecular imaging with femtosecond x-ray pulses", Nature **406**, 6797, 752–757 (2000).

Shvedov, V. G., A. V. Rode, Y. V. Izdebskaya, A. S. Desyatnikov, W. Krolikowski and Y. S. Kivshar, "Giant optical manipulation", Phys. Rev. Lett. **105**, 118103, URL `https://link.aps.org/doi/10.1103/PhysRevLett.105.118103` (2010).

Stegun, I. A. and M. Abramowitz, "Generation of bessel functions on high speed computers", Mathematical Tables and Other Aids to Computation **11**, 60, 255–257 (1957).

Varshalovich, D. A., A. N. Moskalev and V. K. Khersonskii, *Quantum Theory of Angular Momentum* (World Scientific, 1988).

APPENDIX A

HELMHOLTZ EQUATION - DERIVATION FROM MAXWELL'S EQUATIONS

Begin from the complex, position dependent, Maxwell's equations

$$\begin{aligned}
\boldsymbol{\nabla} \cdot \mathbf{E}_c &= 0 \\
\boldsymbol{\nabla} \cdot \mathbf{B}_c &= 0 \\
\boldsymbol{\nabla} \times \mathbf{E}_c &= i\omega \mathbf{B}_c \\
\boldsymbol{\nabla} \times \mathbf{B}_c &= -i\mu_0 \varepsilon_0 \omega \mathbf{E}_c.
\end{aligned}$$

To eliminate $\mathbf{B}_c$, plug the last equation into the penultimate equation.

$$\begin{aligned}
-\frac{i}{\omega} \boldsymbol{\nabla} \times (\boldsymbol{\nabla} \times \mathbf{E}_c) &= -i\mu_0 \varepsilon_0 \omega \mathbf{E}_c \\
\boldsymbol{\nabla} \times (\boldsymbol{\nabla} \times \mathbf{E}_c) &= \mu_0 \varepsilon_0 \omega^2 \mathbf{E}_c \\
\boldsymbol{\nabla} \cdot (\boldsymbol{\nabla} \cdot \mathbf{E}_c) - \nabla^2 \mathbf{E}_c &= \mu_0 \varepsilon_0 \omega^2 \mathbf{E}_c \\
\nabla^2 \mathbf{E}_c &= -\mu_0 \varepsilon_0 \omega^2 \mathbf{E}_c \\
\nabla^2 \mathbf{E}_c &= -k^2 \mathbf{E}_c
\end{aligned}$$

Similarly, to eliminate $\mathbf{E}_c$, plug the penultimate equation into the last equation.

$$\begin{aligned}
-\frac{i}{\mu_0 \varepsilon_0 \omega} \boldsymbol{\nabla} \times (\boldsymbol{\nabla} \times \mathbf{B}_c) &= -i\omega \mathbf{B}_c \\
\boldsymbol{\nabla} \times (\boldsymbol{\nabla} \times \mathbf{B}_c) &= \mu_0 \varepsilon_0 \omega^2 \mathbf{B}_c \\
\boldsymbol{\nabla} \cdot (\boldsymbol{\nabla} \cdot \mathbf{B}_c) - \nabla^2 \mathbf{B}_c &= \mu_0 \varepsilon_0 \omega^2 \mathbf{B}_c \\
\nabla^2 \mathbf{B}_c &= -\mu_0 \varepsilon_0 \omega^2 \mathbf{B}_c \\
\nabla^2 \mathbf{B}_c &= -k^2 \mathbf{B}_c
\end{aligned}$$

APPENDIX B

HELMHOLTZ EQUATION - SEPARATION OF VARIABLES

Assume the solution of

$$\frac{1}{r^2}\frac{\partial}{\partial r}\left(r^2\frac{\partial\psi}{\partial r}\right)+\frac{1}{r^2\sin(\theta)}\frac{\partial}{\partial\theta}\left(\sin(\theta)\frac{\partial\psi}{\partial\theta}\right)+\frac{1}{r^2\sin^2(\theta)}\frac{\partial^2\psi}{\partial\phi^2}+k^2\psi=0$$

is of the form

$$\psi(r,\theta,\phi)=\psi_r(r)\psi_\theta(\theta)\psi_\phi(\phi)$$

Plugging in the solution and multiplying through by

$$\frac{r^2\sin^2(\theta)}{\psi_r\psi_\theta\psi_\phi}$$

we get

$$\frac{\sin^2(\theta)}{\psi_r}\frac{\mathrm{d}}{\mathrm{d}r}\left(r^2\frac{\mathrm{d}\psi_r}{\mathrm{d}r}\right)+\frac{\sin(\theta)}{\psi_\theta}\frac{\partial}{\partial\theta}\left(\sin(\theta)\frac{\mathrm{d}\psi_\theta}{\mathrm{d}\theta}\right)+\frac{1}{\psi_\phi}\frac{\mathrm{d}^2\psi_\phi}{\mathrm{d}\phi^2}+k^2r^2\sin^2(\theta)\psi=0.$$

The ϕ component is now separated, and we must conclude that it is equal to some constant

$$\frac{1}{\psi_\phi}\frac{\mathrm{d}^2\psi_\phi}{\mathrm{d}\phi^2}=-m^2.$$

The last two components,

$$\frac{\sin^2(\theta)}{\psi_r}\frac{\mathrm{d}}{\mathrm{d}r}\left(r^2\frac{\mathrm{d}\psi_r}{\mathrm{d}r}\right)+k^2r^2\sin^2(\theta)\psi=\frac{\sin(\theta)}{\psi_\theta}\frac{\partial}{\partial\theta}\left(\sin(\theta)\frac{\mathrm{d}\psi_\theta}{\mathrm{d}\theta}\right)-m^2,$$

can be separated by dividing through by $\sin^2(\theta)$.

$$\frac{1}{\psi_r}\frac{\mathrm{d}}{\mathrm{d}r}\left(r^2\frac{\mathrm{d}\psi_r}{\mathrm{d}r}\right)+k^2r^2\psi=\frac{1}{\psi_\theta\sin(\theta)}\frac{\partial}{\partial\theta}\left(\sin(\theta)\frac{\mathrm{d}\psi_\theta}{\mathrm{d}\theta}\right)-\frac{m^2}{\sin^2(\theta)}$$

Again we are lead to conclude that the two components are equal to some constant

$$\frac{\mathrm{d}}{\mathrm{d}r}\left(r^2\frac{\mathrm{d}\psi_r}{\mathrm{d}r}\right)+\left[k^2r^2-\ell(\ell+1)\right]\psi_r=0$$

$$\frac{1}{\sin(\theta)}\frac{\partial}{\partial\theta}\left(\sin(\theta)\frac{\mathrm{d}\psi_\theta}{\mathrm{d}\theta}\right)+\left[\ell(\ell+1)-\frac{m^2}{\sin^2(\theta)}\right]\psi_\phi=0.$$

APPENDIX C

INTERNAL AND SCATTERED FIELD EXPANSION COEFFICIENTS

The expansion coefficients for the internal and scattered field come from the boundary conditions

$$\left[\mathbf{E}_0(\mathbf{r}) + \mathbf{E}_s(\mathbf{r}) - n^2(r)\mathbf{E}_i(\mathbf{r})\right] \cdot \hat{\mathbf{r}} = 0 \tag{C.1}$$

$$\left[\mathbf{B}_0(\mathbf{r}) + \mathbf{B}_s(\mathbf{r}) - \mathbf{B}_i(\mathbf{r})\right] \cdot \hat{\mathbf{r}} = 0 \tag{C.2}$$

$$\left[\mathbf{E}_0(\mathbf{r}) + \mathbf{E}_s(\mathbf{r}) - \mathbf{E}_i(\mathbf{r})\right] \times \hat{\mathbf{r}} = 0 \tag{C.3}$$

$$\left[\mathbf{B}_0(\mathbf{r}) + \mathbf{B}_s(\mathbf{r}) - \mathbf{B}_i(\mathbf{r})\right] \times \hat{\mathbf{r}} = 0. \tag{C.4}$$

Theorem C.0.1.

$$\mathbf{M}_{\ell,m} \cdot \hat{\mathbf{r}} = 0 \tag{C.5}$$

and

$$\mathbf{N}_{\ell,m} \cdot \hat{\mathbf{r}} = \frac{z_\ell(kr)}{kr}\ell(\ell+1)Y_{\ell,m}(\theta,\phi). \tag{C.6}$$

Proof. From eqs. (3.18) and (4.23) we conclude

$$\begin{aligned}
\mathbf{M}_{\ell,m} \cdot \hat{\mathbf{r}} &= i\mathbf{L} \cdot \hat{\mathbf{r}}\ \psi_{\ell,m} \\
&= (\mathbf{r} \times \boldsymbol{\nabla}) \cdot \hat{\mathbf{r}}\ \psi_{\ell,m} \\
&= (\hat{\mathbf{r}} \times \boldsymbol{\nabla}) \cdot \hat{\mathbf{r}}\ r\psi_{\ell,m} \\
&= 0
\end{aligned}$$

and

$$\begin{aligned}
\mathbf{N}_{\ell,m} \cdot \hat{\mathbf{r}} &= \frac{r}{r}\frac{i}{k}\left[\boldsymbol{\nabla} \times \mathbf{L}\right] \cdot \hat{\mathbf{r}}\ \psi_{\ell,m} \\
&= \frac{i}{kr}\left[\boldsymbol{\nabla} \times \mathbf{L}\right] \cdot \mathbf{r}\ \psi_{\ell,m} \\
&= \frac{i}{kr}\left[\mathbf{r} \times \boldsymbol{\nabla}\right] \cdot \mathbf{L}\ \psi_{\ell,m} \\
&= -\frac{i^2}{kr}L^2\psi_{\ell,m} \\
&= \frac{z_\ell(kr)}{kr}\ell(\ell+1)Y_{\ell,m}(\theta,\phi).
\end{aligned}$$

□

$$\begin{aligned}
0 &= \left[\mathbf{E}_0(\mathbf{r}) + \mathbf{E}_s(\mathbf{r}) - n^2(r)\mathbf{E}_i(\mathbf{r})\right] \cdot \hat{\mathbf{r}} \\
&= \frac{1}{kr}\left[\beta^0_{\ell,m}j_\ell(kr) + \beta^s_{\ell,m}h^{(1)}_\ell(kr) - n^2(r)\beta^i_{\ell,m}j_\ell(knr)\right]\ell(\ell+1)Y_{\ell,m}(\theta,\phi) \\
&= \beta^0_{\ell,m}j_\ell(kr) + \beta^s_{\ell,m}h^{(1)}_\ell(kr) - n^2(r)\beta^i_{\ell,m}j_\ell(knr)
\end{aligned}$$

$$\begin{aligned}
0 &= \left[\mathbf{B}_0(\mathbf{r}) + \mathbf{B}_s(\mathbf{r}) - \mathbf{B}_i(\mathbf{r})\right] \cdot \hat{\mathbf{r}} \\
&= \frac{1}{kr}\left[\alpha^0_{\ell,m}j_\ell(kr) + \alpha^s_{\ell,m}h^{(1)}_\ell(kr) - \alpha^i_{\ell,m}j_\ell(knr)\right]\ell(\ell+1)Y_{\ell,m}(\theta,\phi) \\
&= \alpha^0_{\ell,m}j_\ell(kr) + \alpha^s_{\ell,m}h^{(1)}_\ell(kr) - \alpha^i_{\ell,m}j_\ell(knr)
\end{aligned}$$

Using

$$\boldsymbol{\nabla} \times z_\ell(kr)\mathbf{L}Y_{\ell,m}(\theta,\phi) = \frac{i}{r} z_\ell(kr) Y_{\ell,m}(\theta,\phi)\hat{\mathbf{r}} + \frac{1}{r}\frac{\partial}{\partial r}\left[r z_\ell(kr)\right]\hat{\mathbf{r}} \times \mathbf{L}Y_{\ell,m}(\theta,\phi), \quad \text{(C.7)}$$

Jackson (1999), to rewrite

$$\mathbf{E} = \sum_{\ell,m}\left[\alpha_{\ell,m} i\mathbf{L} + \beta_{\ell,m}\frac{i}{k}\boldsymbol{\nabla}\times\mathbf{L}\right] z_\ell(kr) Y_{\ell,m}(\theta,\phi)$$

as

$$\mathbf{E} = \sum_{\ell,m}\left[\alpha_{\ell,m} i\mathbf{L} - \beta_{\ell,m}\frac{1}{kr}\hat{\mathbf{r}} + \beta_{\ell,m}\frac{i}{kr}\frac{\partial}{\partial r}\left[r\right]\hat{\mathbf{r}}\times\mathbf{L}\right] z_\ell(kr) Y_{\ell,m}(\theta,\phi)$$

and doing the same for $\mathbf{B}$ we can write the last two boundary conditions.

$$\begin{aligned}
0 &= \left[\mathbf{E}_0(\mathbf{r}) + \mathbf{E}_s(\mathbf{r}) - \mathbf{E}_i(\mathbf{r})\right]\times\hat{\mathbf{r}} \\
&= \left[\alpha^0_{\ell,m}\mathbf{M}^0_{\ell,m} + \beta^0_{\ell,m}\mathbf{N}^0_{\ell,m} + \alpha^s_{\ell,m}\mathbf{M}^s_{\ell,m} + \beta^s_{\ell,m}\mathbf{N}^s_{\ell,m} - \alpha^i_{\ell,m}\mathbf{M}^i_{\ell,m} - \beta^i_{\ell,m}\mathbf{N}^i_{\ell,m}\right]\times\hat{\mathbf{r}} \\
&= i\left[\alpha^0_{\ell,m} j_\ell(kr) + \alpha^s_{\ell,m} h^{(1)}_\ell(kr) - \alpha^i_{\ell,m} j_\ell(knr)\right]\mathbf{L}Y_{\ell,m}(\theta,\phi) \\
&\quad - \frac{1}{kr}\left[\beta^0_{\ell,m} j_\ell(kr) + \beta^s_{\ell,m} h^{(1)}_{\ell,m}(kr) - \beta^i_{\ell,m} j_\ell(knr)\right]\hat{\mathbf{r}} \\
&\quad + \frac{i}{kr}\frac{\partial}{\partial r}\left[\beta^0_{\ell,m} r j_\ell(kr) + \beta^s_{\ell,m} r h^{(1)}_{\ell,m}(kr) - \beta^i_{\ell,m} r j_\ell(knr)\right]\hat{\mathbf{r}}\times\mathbf{L}Y_{\ell,m}(\theta,\phi)
\end{aligned}$$

$$\begin{aligned}
0 &= \left[\mathbf{B}_0(\mathbf{r}) + \mathbf{B}_s(\mathbf{r}) - \mathbf{B}_i(\mathbf{r})\right]\times\hat{\mathbf{r}} \\
&= \left[\alpha^0_{\ell,m}\mathbf{N}^0_{\ell,m} + \beta^0_{\ell,m}\mathbf{M}^0_{\ell,m} + \alpha^s_{\ell,m}\mathbf{N}^s_{\ell,m} + \beta^s_{\ell,m}\mathbf{M}^s_{\ell,m} - \alpha^i_{\ell,m}\mathbf{N}^i_{\ell,m} - \beta^i_{\ell,m}\mathbf{M}^i_{\ell,m}\right]\times\hat{\mathbf{r}} \\
&= i\left[\beta^0_{\ell,m} j_\ell(kr) + \beta^s_{\ell,m} h^{(1)}_\ell(kr) - \beta^i_{\ell,m} j_\ell(knr)\right]\mathbf{L}Y_{\ell,m}(\theta,\phi) \\
&\quad - \frac{1}{kr}\left[\alpha^0_{\ell,m} j_\ell(kr) + \alpha^s_{\ell,m} h^{(1)}_{\ell,m}(kr) - \alpha^i_{\ell,m} j_\ell(knr)\right]\hat{\mathbf{r}} \\
&\quad + \frac{i}{kr}\frac{\partial}{\partial r}\left[\alpha^0_{\ell,m} r j_\ell(kr) + \alpha^s_{\ell,m} r h^{(1)}_{\ell,m}(kr) - \alpha^i_{\ell,m} r j_\ell(knr)\right]\hat{\mathbf{r}}\times\mathbf{L}Y_{\ell,m}(\theta,\phi)
\end{aligned}$$

Now we rewrite the boundary conditions as

$$\begin{aligned}
\alpha^0_{\ell,m} j_\ell(kr) &= \alpha^i_{\ell,m} j_\ell(knr) - \alpha^s_{\ell,m} h^{(1)}_\ell(kr) \\
\beta^0_{\ell,m} j_\ell(kr) &= n^2(r)\beta^i_{\ell,m} j_\ell(knr) - \beta^s_{\ell,m} h^{(1)}_\ell(kr)
\end{aligned}$$

and

$$\begin{aligned}
0 &= \alpha^0_{\ell,m}\frac{\partial}{\partial r}\left[r j_\ell(kr)\right] + \alpha^s_{\ell,m}\frac{\partial}{\partial r}\left[r h^{(1)}_{\ell,m}(kr)\right] - \alpha^i_{\ell,m}\frac{\partial}{\partial r}\left[r j_\ell(knr)\right] \\
&= \beta^0_{\ell,m}\frac{\partial}{\partial r}\left[r j_\ell(kr)\right] + \beta^s_{\ell,m}\frac{\partial}{\partial r}\left[r h^{(1)}_{\ell,m}(kr)\right] - \beta^i_{\ell,m}\frac{\partial}{\partial r}\left[r j_\ell(knr)\right].
\end{aligned}$$